THE EXIT CHART – INTRODUCTION TO EXTRINSIC INFORMATION TRANSFER IN ITERATIVE PROCESSING

Joachim Hagenauer

Institute of Communications Engineering (LNT), Munich University of Technology (TUM)
Arcisstraße 21, D-80290 München, Germany
phone: +49 89 28923467, fax: +49 89 28923467, email: hagenauer@ei.tum.de
web: www.lnt.ei.tum.de

ABSTRACT

The extrinsic information transfer (EXIT) chart pioneered by Stephan ten Brink is introduced in a tutorial way for readers not yet familiar with this powerful technique which is used to analyze the behavior of iterative so-called turbo techniques. Simple examples and preliminary analytical results are given as well as some typical applications.

1. THE TURBO PRINCIPLE

The 'Turbo-Principle', originally invented for decoding of concatenated codes [2], [3] is a general principle in decoding and detection and can be applied to many detection/decoding problems such as parallel or serial concatenation, equalization, coded modulation, multiuser detection, multiple-input/multiple-output (MIMO) detection, joint source and channel decoding, low density parity check (LDPC) decoding and others. In many cases we can describe the system as a serial concatenation as shown for a few examples in Fig.1. For example in a simple mobile system the inner 'encoder' would be the multipath channel. The crucial point at the receiver is that the two detectors/decoders are soft-in/soft-out decoders that accept and deliver probabilities or soft values and the extrinsic part of the soft-output of one decoder is passed on to the other decoder to be used as a priori input. This principle has been applied for the first time to decoding of two dimensional product-like codes [2] and other concatenated codes [3]. Berrou's application is sometimes called a 'turbo code. Strictly speaking there is nothing 'turbo' in the codes. Only the decoder uses a 'turbo' feedback. This

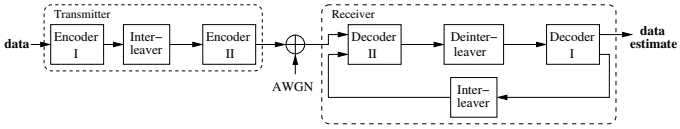

configuration	en-/decoder I (outer code)	en-/decoder II (inner code)
serial code concat.	FEC en-/decoder	FEC en-/decoder
turbo equalization	FEC en-/decoder	Multipath channel/detector
turbo BiCM	FEC en-/decoder	Mapper/demapper
turbo DPSK	FEC en-/decoder	Precoder
turbo MIMO	FEC en-/decoder	Mapper & MIMO detector
turbo source-channel	source encoder	FEC en-/decoder
LDPC code/decoder	check nodes	variable nodes

Figure 1: A serial concatenated system with iterative detection/decoding.

Invited Tutorial Paper. The author would like to thank Michael Tüchler and Frank Schreckenbach for simulating some of the charts in this paper.

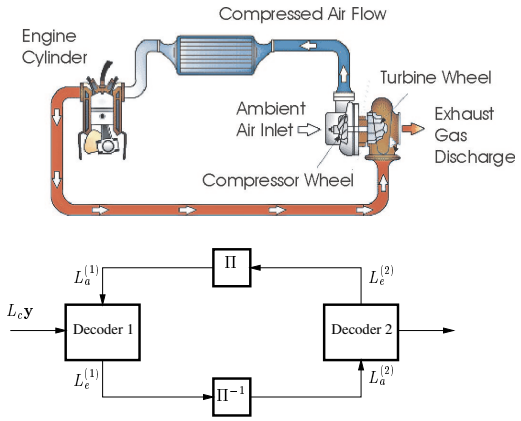

Figure 2: A mechanical turbo engine and a turbo decoder.

is similar as in a mechanical turbo engine which is shown in Fig.2. In the same way as the compressed air is fed back from the compressor to the main engine the extrinsic information is fed back to the other decoder. This constitutes an iterative process with an information transfer between the two decoders which is not easy to analyze and to describe. One very useful tool is the **EX**trinsic **I**nformation **T**ransfer **EXIT** chart introduced by Stephan ten Brink [1].

2. MUTUAL INFORMATION AND EXIT CHARTS

2.1 Shannon's Mutual Information

Let X and Y be two real valued random variables. Then Shannon's mutual information is defined as

$$I(X;Y) = \int\int f(x,y)\log\frac{f(x,y)}{f(x)\cdot f(y)}\,dxdy$$

with

$$I(X;Y) = H(Y) - H(Y|X)$$

where

$$H(Y|X) = \int\int f(x,y)\log\frac{1}{f(y|x)}\,dxdy$$

For an additive channel with $Y = X + Z$ with statistically independent Z

$$H(Y|X) = H(Z)$$

With the transmit power $P_x = {\sigma_x}^2 = E_s\cdot(1/T)$, the noise power $P_n = {\sigma_n}^2 = {\sigma_z}^2 = (N_0/2)\cdot(1/T)$ and the receive

power $P_y = {\sigma_y}^2 = {\sigma_x}^2 + {\sigma_n}^2 = P_y = P_x + P_n$ we have

$$I(X;Y) = H(Y) - H(Z)$$

$$I(X;Y) \leq \frac{1}{2}\log(1+\frac{P_x}{P_n})$$

$$I(X;Y) \leq \frac{1}{2}\log(1+\frac{2E_s}{N_0})$$

the mutual information of the AWGN channel with equality for Gaussian input. For Gaussian input and noise the output becomes also Gaussian and the capacity is achieved:

$$C = \max_{f(X)} I(X;Y) = \frac{1}{2}\log(1+\frac{2E_s}{N_0})$$

If we restrict ourselves to binary inputs with $x \in \{+1,-1\}$ the mutual information becomes

$$I(X;Y) = \sum_{x=+1,-1} \int_{-\infty}^{+\infty} f(y|x)P(x)\log\frac{f(y|x)}{f(y)}\,dy \qquad (1)$$

and the maximal mutual information is achieved for equally likely inputs x as

$$I(X;Y) = \frac{1}{2}\sum_{x=+1,-1} \int_{-\infty}^{+\infty} f(y|x)\log\frac{f(y|x)}{f(y)}dy \qquad (2)$$

with

$$f(y) = \frac{1}{2}(f(y|x=+1) + f(y|x=-1)) \qquad (3)$$

and

$$f(y|x=\pm 1) = \frac{1}{\sqrt{2\pi}\sigma} e^{-\frac{(y\mp 1)^2}{2\sigma^2}} \qquad (4)$$

where $\sigma^2 = N_0/(2E_s)$. The integral has to be evaluated numerically and has the performance shown in Fig.3. Loosely speaking it shows how much of a bit is known after transmission over a noisy channel.

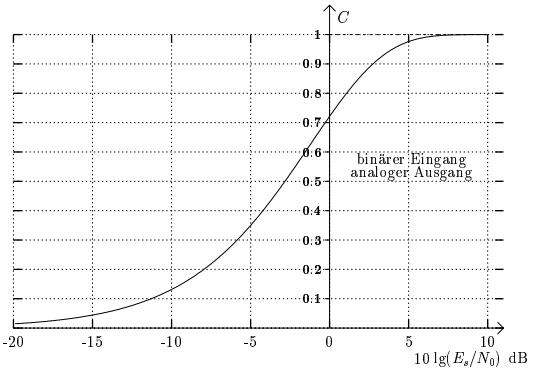

Figure 3: Binary mutual information as a function of the SNR in dB.

2.2 Log-Likelihood Values and the Consistency Condition

Let u be in GF(2) with the elements $\{+1,-1\}$, where $+1$ is the 'null' element under the $\oplus$ addition. Then the **log-likelihood ratio (LLR)** or L-value [4] of the binary random variable (r.v.) is [1]

$$L(u) = \ln\frac{P(u=+1)}{P(u=-1)} \qquad (5)$$

with the inverse

$$P(u=\pm 1) = \frac{e^{\pm L(u)/2}}{e^{+L(u)/2} + e^{-L(u)/2}}. \qquad (6)$$

The sign of $L(u)$ is the hard decision and the magnitude $|L(u)|$ is the reliability of this decision.
We define the **soft bit** $\lambda(u)$ as the expectation of u where we simultaneously view u in GF(2) and as an integer number

$$\begin{aligned}\lambda(u) = \mathrm{E}\{u\} &= (+1)\cdot P(u=+1) + (-1)\cdot P(u=-1) \\ &= \tanh(L(u)/2). \qquad (7)\end{aligned}$$

If $P(u)$ is a random variable in the range of (0,1) then $L(u)$ is a r.v. in the range $(-\infty,+\infty)$ and $\lambda(u)$ a r.v. in the range (-1,+1). The GF(2) addition $u_1 \oplus u_2$ of two independent binary random variables transforms into $\mathrm{E}\{\mathrm{u}_1\cdot\mathrm{u}_2\} = \mathrm{E}\{\mathrm{u}_1\}\mathrm{E}\{\mathrm{u}_2\} = \lambda(u_1)\cdot\lambda(u_2)$. Therefore the L value of the sum $L(u_1 \oplus u_2)$ equals

$$2\tanh^{-1}(\tanh(L(u_1)/2)\cdot\tanh(L(u_2)/2)) = L(u_1)\boxplus L(u_2),$$

abbreviated by the **boxplus operation** $\boxplus$.

The a posteriori probability (APP) after transmitting x over a noisy multiplicative fading channel with amplitude a yielding $y = ax+n$ and the Gaussian probability density function

$$p(y|x) = \frac{1}{\sqrt{2\pi\sigma_c^2}} e^{\frac{-(y-ax)^2}{2\sigma_c^2}} \qquad (8)$$

is

$$P(x|y) = \frac{p(y|x)P(x)}{p(y)} \qquad (9)$$

and the complementary APP LLR equals

$$L_{CH} = L(x|y) = \ln\frac{P(x=+1|y)}{P(x=-1|y)} = L_c\cdot y + L(x). \qquad (10)$$

$L(x)$ is the a priori LLR of x and L_c is the channel state information (CSI):

$$L_c = \frac{2a}{\sigma_c^2} = 4aE_s/N_0 \qquad (11)$$

The matched filter output y is Gaussian with $\mathcal{N}(m,\sigma_c^2) = \mathcal{N}(\pm 2a,\sigma_c^2)$. Further, the APP LLR L_{CH} is also Gaussian with $\mathcal{N}(\pm\sigma_{CH}^2/2,\sigma_{CH}^2)$ where $\sigma_{CH}^2 = 2aL_c$ and is determined by one parameter. Note, that the matched filter output has a symmetric pdf $p(-y|x=+1) = p(y|x=-1)$ and

[1] For simplicity of notation henceforward we do not strictly distinguish between the r.v. capital U and its realization or integration variable small u

is a LLR and as all true LLR with symmetric distributions satisfies the **consistency condition**

$$p(-y|x) = e^{-L_c xy} p(y|x). \tag{12}$$

We further note that for statistically independent transmission, as in dual diversity or with a repetition code

$$L(x|y_1, y_2) = L_{c_1} y_1 + L_{c_2} y_2 + L(x). \tag{13}$$

The mutual information between the equally likely X and the respective LLR's L for symmetric and consistent L-values simplifies to

$$I(L;X) = 1 - \int_{-\infty}^{+\infty} p(L|x=+1) \log_2(1+e^{-L}) dL \tag{14}$$

$$I(L;X) = 1 - \mathrm{E}\{\log_2(1+e^{-L})\} \tag{15}$$

The expectation is over the one parameter distribution

$$p(L|x=+1) = \frac{1}{\sqrt{2\pi\sigma^2}}\, e^{-(L-x\sigma^2/2)^2/2\sigma^2} \tag{16}$$

The nonlinearity can be also expressed as

$$\begin{aligned} 1 - \mathrm{E}\{\log_2(1+e^{-L})\} &= \mathrm{E}\{\log_2(1+\tanh(L/2))\} \\ &= \mathrm{E}\{\log_2(1+\lambda)\} \end{aligned} \tag{17}$$

If the input values are not equally likely ($P(x) \neq 1/2$ resp. $L(x) \neq 0$ then (15) generalizes to

$$I(L;X) = H_b(P(x) - \mathrm{E}\{\log_2(1+e^{-L})\} \tag{18}$$

where H_b is the binary entropy function.

2.3 Measurement of Mutual Information and the Test (A Priori) Channel

We wish to measure the mutual between information bits x which after encoding are transmitted over a noisy channel and the L-values (soft output) of these bits after decoding. The decoder receives not only the transmitted values normalized by the channel state information but also a priori knowledge in the form of L-values from the other serial or parallel decoding engine. This is shown by the lower input line to the decoder in Fig.4 . Due to the nonlinearity of the decoder the L-value distribution of the output is in general unknown and no longer Gaussian. However, by invoking the ergodicity theorem – namely that the expectation can be replaced by the time average – we can measure the mutual information from a large number N of samples even for non-Gaussian or unknown distributions:

$$I(L;X) = 1 - \mathrm{E}\{\log_2(1+e^{-L})\} \approx 1 - \frac{1}{N}\sum_{n=1}^{N} \log_2(1+e^{-x_n \cdot L_n})$$

The N decoder output samples are corrected by x_n to account for the pdf over positive x. Even this knowledge of x_n is not necessary [5] if one observes that we can write $L_n = \mathrm{sgn}(L_n) \cdot |L_n|$. An error $x_n \cdot \mathrm{sgn}(L_n) = -1$ occurs with probability (relative frequency) of

$$P_{e_n} = \frac{e^{+|L_n)|/2}}{e^{+|L_n|/2} + e^{-|L_n|/2}}.$$

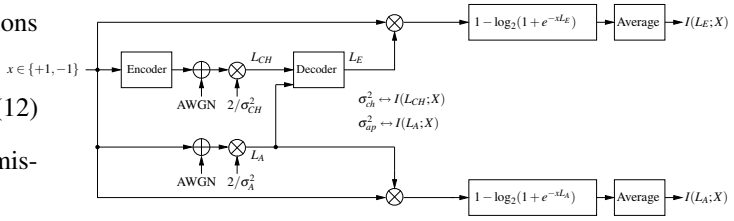

Figure 4: Measurement of the EXIT chart

This leads to

$$I(L;X) \approx 1 - \frac{1}{N}\sum_{n=1}^{N} H_b(P_{e_n}) = 1 - \frac{1}{N}\sum_{n=1}^{N} H_b\left(\frac{e^{+|L_n)|/2}}{e^{+|L_n|/2} + e^{-|L_n|/2}}.\right)$$

This new nonlinear transformation and the averaging of the $|L_n|$ values allows us to estimate the mutual information only from the magnitudes without knowing the correct data.
The lower part of the diagram in Fig.4 is the **a priori** or **test** channel which supplies the a priori L-values to the decoder. It models the nonlinear performance of the mutually other decoder in the turbo scheme of Fig.2. For the modelling of the test channel we have several options:

- Model it as an AWGN channel (see previous Fig.4). This was ten Brinks original assumption. He considered the soft output of the other constituent decoder to be a consistent normally distributed LLR.
- Model it as a BEC with erasure probability ε. Here we assume the other constituent decoder to be a genie aided decoder which converts errors into erasures. This genie aided decoder is the optimal (however unrealizable) SISO decoder. Hereby we replace the AWGN a priori channel by a multiplicative channel with an i.i.d. factor

  $$a_n = \begin{cases} \infty & \text{with probability} \quad 1-\varepsilon \\ 0 & \text{with probability} \quad \varepsilon \end{cases}$$

  Then the mutual information becomes for large N

  $$I(L;X) = 1 - \frac{1}{N}\sum_{n=1}^{N} \log_2(1+e^{-a_n}) = 1 - \varepsilon$$

  as it should be for the BEC.
- Model it as a BSC with crossover probability P_0 . Then the channel is multiplicative channel with an i.i.d. factor

  $$a_n = \begin{cases} \ln\frac{1-P_0}{P_0} & \text{with probability} \quad 1-P_0 \\ -\ln\frac{1-P_0}{P_0} & \text{with probability} \quad P_0 \end{cases}$$

  Then the mutual information becomes for large N

  $$I(L;X) = 1 - \frac{1}{N}\sum_{n=1}^{N} \log_2(1+e^{-a_n}) = 1 - H_b(P_0)$$

  as it should be for the BSC.

All the model test channels produce i.i.d. variables which is achieved in a real system by applying interleaving with a large blocksize.

2.4 The Exit Chart

Pioneered by Stephan ten Brink the information transfer for turbo decoding and the performance of turbo decoding in the fall-off region can be visualized by the EXIT Chart. It plots the mutual information of the constituent decoder number one versus the mutual information of the other constituent decoder (number two) which is modelled by the test (a priori) channel. In other words the output of the lower branch in in Fig.4 determines the value of the horizontal axis of the EXIT chart and the output of the upper branch determines the value on the vertical axis. Both range between 0 and 1. For the next (half) iteration both decoders are swapped and interchange their roles: The output of decoder one becomes the a priori input of decoder number two. This allows the separate investigation and optimization of each constituent code. Only the extrinsic L-values L_E are used as output, meaning that the a priori input value is subtracted from the full (APP) soft-output L-value. This avoids propagation of already known information.
The information transfer function T is measured as

$$I(L_E;X) = T(I(L_A;X)) \tag{19}$$

with the following provisions:

- The assumption is a large interleaver to assure statistical independence and in the original form of model one assumes a Gaussian distribution for the input L_A with parameter $\sigma_a^2 \leftrightarrow I(L_A;X)$.
- For inner decoders in a serial concatenated scheme and for parallel concatenated schemes the additional parameter input is L_{CH} and σ_{CH}^2, the channel SNR or $I(L_{CH};X)$ appears as parameter on a set of EXIT curves.
- For outer decoders in a serial concatenation only $L_A^{(o)}$ appears as input which is taken from the interleaved serial $L_E^{(i)}$.

2.5 Measured and Analytical Results for Exit Charts of Simple Single Parity Check (SCPC) Codes

We will give an example for a parallel concatenated system with single parity check component codes SPC with parameters (n-1, n, d=2) on the AWGN channel. Assume an (2,3,2) SPC code with a codeword $(+1,+1,+1)$ and decoded with an a priori information at $I(L_A;X) \to 1$.
With the use of the boxplus function we obtain for bit $x_1 = x_2 \oplus x_3$ the extrinsic value as

$$L_E = (L_{CH,2} + L_A) \boxplus L_{CH,3}.$$

The transfer function eqn.(19) is shown in Figure 5. Note that even for perfect a priori information $I(L_A;X) = 1$ the extrinsic output $I(L_E;X)$ needs not to be 1. For parallel concatenated turbo decoding the axes are swapped and the iteration alternates between the two swapped curves in Figure 5. The difference $I(L_E;X) - I(L_A;X)$ meaning the difference to the diagonal is the average information gain measured in bits per half iteration. The iteration stops if no more information gain is achievable, in the case of such a simple code and low SNR rather early at the point (0.66,0.66). In the case of a good code we should reach the point (1,1) and decode virtually errorfree. A more sophisticated example with measured EXIT charts is shown in Fig.6. The upper DPSK curve reaches the point (1,1). Its APP decoder uses a two

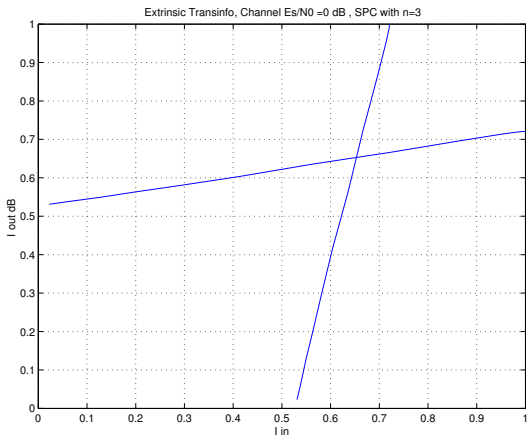

Figure 5: EXIT Chart for a parallel concatenated (3,2,2) SPC code at a channel SNR of 0 dB.

state trellis. Since the interleaver is limited to 50000 bits the actual trajectory differs slightly from two EXIT curves. Only very limited analytical results are available for and the

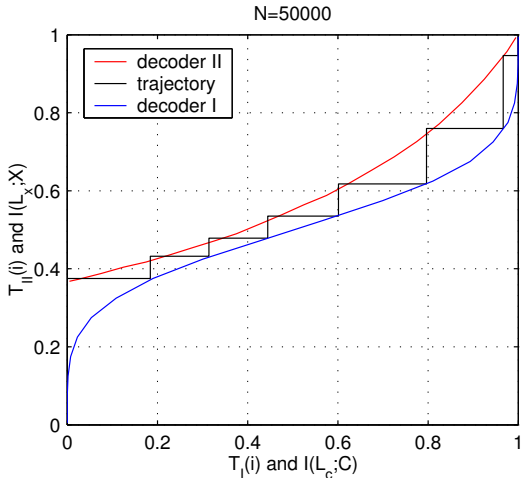

Figure 6: Serial concatenation with a DPSK modulator as inner code and an outer $M = 2$ convolutional code, $R = 1/2$ at an E_b/N_0 of 1.5 dB

EXIT transfer functions on the AWGN channel. We give here one simple example again with the SCPC code: Assume the (2,3,2) SPC code with codeword $(+1,+1,+1)$ and decode at $I(L_A;X) \to 1$. Use the boxplus function to obtain

$$\begin{aligned} L(x_1 \oplus x_2) &= L(x_1) \boxplus L(x_2) \\ &= 2\tanh^{-1}(\tanh(L(x_1)) \cdot \tanh(L(x_2)) \\ &\approx \operatorname{sign}(L(x_1)) \cdot \operatorname{sign}(L(x_2) \cdot \min\left(|L(x_1)|, |L(x_1)|\right). \end{aligned}$$

For bit $x_1 = x_2 \oplus x_3$ the extrinsic value is assuming no decoding error

$$L_E = (L_{CH,2} + L_A) \boxplus L_{CH,3} \approx \min\left(L_{CH,2} + L_A, L_{CH,3}\right) \approx L_{CH,3}$$

The last approximation is true because L_A is much larger than $L_{CH,n}$. Therefore with Jensen's inequality we obtain

$$\begin{aligned} I(L_E;X) &= 1-\mathrm{E}\{\log_2(1+e^{-L_E})\} \\ &\approx 1-\log_2(1+e^{-\mathrm{E}\{L_{CH}\}}) \\ &= 1-\log_2(1+e^{-4E_s/N_0}) \end{aligned} \quad (20)$$

the following values for the rightmost EXIT chart value

E_S/N_0	simulation	calculation
-5 dB	0.92	0.92
0 dB	0.72	0.72
3 dB	0.35	0.36

Closed form solutions for EXIT charts are available only for erasure transmission channels and erasure test channels and only for simple codes. Recently Ingmar Land et.al. [6] were able to calculate very good upper and lower analytical bounds again for SPC and repetition codes which however are valid for any channel.

2.6 Rate-Capacity Properties of EXIT Charts for Serially Concatenated Schemes.

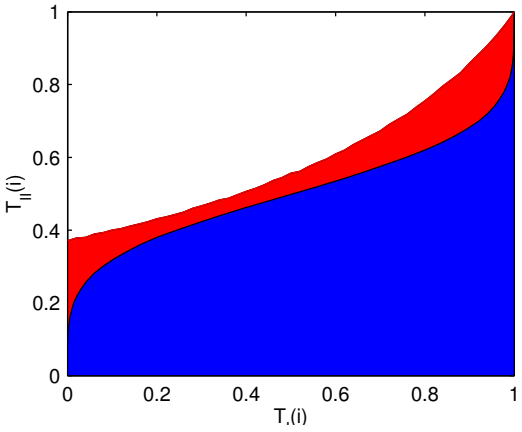

Figure 7: Rate-Capacity Relation of the EXIT charts where the rate of the inner scheme is $R_{\mathrm{II}} = 1$

For a serially concatenated scheme as shown in Fig.1 where the inner code II is a rate 1 code, such as a multipath channel in turbo equalization or in DPSK encoding the following properties of the EXIT charts in Fig.7 hold:
Capacity property: If the rate of the inner code $R_{II} = 1$ then the area under the white area is

$$\int_0^1 T_{II}(i)\mathrm{d}i \approx C_{ui}$$

Rate property: If the outer decoder I is APP based then the area under the lower (swapped, inverted) curve is

$$\int_0^1 T_I^{-1}(i)\mathrm{d}i \approx R_I$$

If the area between the two curves is

$$\int_0^1 (T_{II}(i)-T_I^{-1}(i))\,\mathrm{d}i > 0 \;\Rightarrow\; R_I < C_{ui}$$

and if the two curves do not intersect the turbo decoder can decode iteratively, then the area property of the EXIT chart is another form of Shannon's capacity theorem stating that the code rate of the outer code has to be smaller than the capacity of the inner channel. These properties were first proven by Ashikhmin, Kramer, ten Brink [10] for an a priori channel with a BEC model and later for an AWGN model .

3. APPLICATIONS OF EXIT CHARTS

From a variety of possible applications we will give only one example for an outer code and one example for an inner "code", namely QAM mapping and precoding.

3.1 Regular and Irregular Convolutional Codes

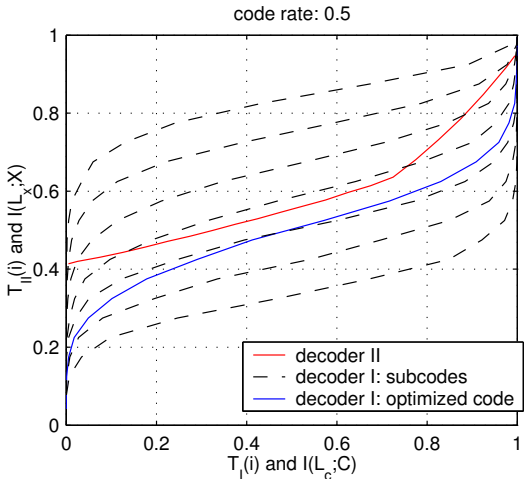

Figure 8: EXIT charts of a coded system with 7 convolutional codes as outer codes and a multipath transmission as inner code

Let us assume a serial concatenation with an outer convolutional code. For this outer FEC coder we use a family of punctured convolutional codes with memory 4 and $L_R = 7$ rates (4/12, 5/12, 6/12, 7/12, 8/12, 9/12, 10/12). Their EXIT charts are given as dotted lines in Figure 8 and start with a value (0,0) because the outer decoder has only one input from the inner decoder. Assume a certain EXIT chart for the inner system (decoder II, here the APP equalizer of a multipath channel [11])at a certain channel SNR which gives already a starting value even with an a priori input zero. Then Figure 8 shows that the rate 1/2 code (5th dotted line from top) cannot achieve convergence in the iterations because the EXIT curves intersect. However we can construct an irregular code with the same average rate 1/2 as indicated in Figure 9. We

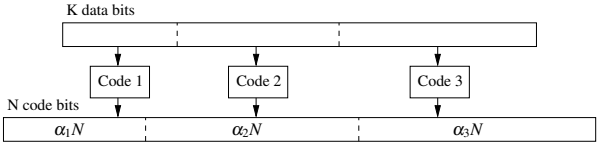

Figure 9: Construction of an irregular code

have the following constraints on the α_k in this FEC code:

$$\sum_{k=1}^{L_R} \alpha_k = 1,$$

$$\sum_{k=1}^{L_R} \alpha_k R_k = 1/2, \text{ and } \alpha_k \in [0,1],\ k = 1,...,L_R.$$

Since the L-values of all subcode decoders are symmetric and consistent the overall transfer function is the sum of the individual EXIT transfer curves.

$$T(i) = \sum_{k=1}^{L_R} \alpha_k T_k(i).$$

By optimizing the set $\{\alpha_i\}$ in such a way that the curves I and II are as close as possible but do not cross in order to keep a reasonable open tunnel for the iterations [13] we obtain the solid curve I in Figure 8.

3.2 QAM Mappings

As a turbo application we consider a QAM system with a memory 2, rate 1/2 outer channel code as shown in Fig.10. This is a so-called bit-interleaved coded modulation system (BICM). If the mapping of the QAM is selected in a proper way the a priori information of the other bits $L_a^d(\mathbf{c})$ can improve the detection of the current bit even no explicit memory is contained. This is shown for a 16-QAM system in

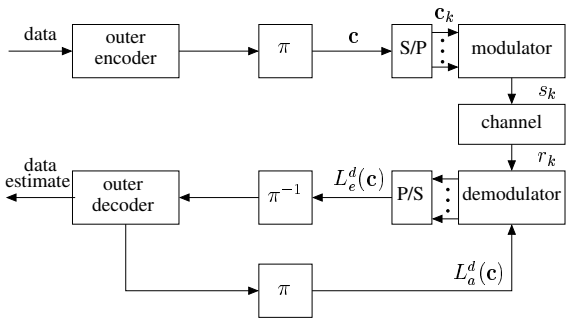

Figure 10: Coded system with a convolutional codes as outer code and a QAM transmission as inner code, bit-interleaved coded modulation BICM.

Fig.11. The Gray mapping does not give any gain with increasing a priori mutual information and iterations do not gain anything. However with other mappings (modified set partitioning MSP and maximum Euclidean weight MSEW, as discussed in [16]) the EXIT charts although starting at a lower value become tilted and iterations become possible as shown in the example trajectory of Fig.11, taken from [16]. The iterations finally lead to a higher extrinsic mutual information. Note however that they do not reach the point (1,1) in the EXIT chart. A remedy against this unwanted behavior is a rate 1 differential precoder as applied in Fig.12. Now after 9 iterations the turbo decoder reaches the full information point $(I_A, I_E) = (1.0, 1.0)$ leading to a low BER although the tunnel is quite narrow.

Further details on iterative QAM systems will be given in a companion paper in this session.

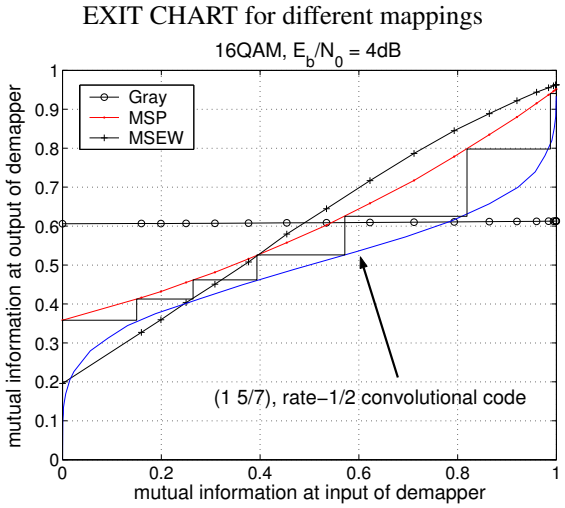

Figure 11: EXIT charts for different QAM mappings as inner code in a BICM scheme.

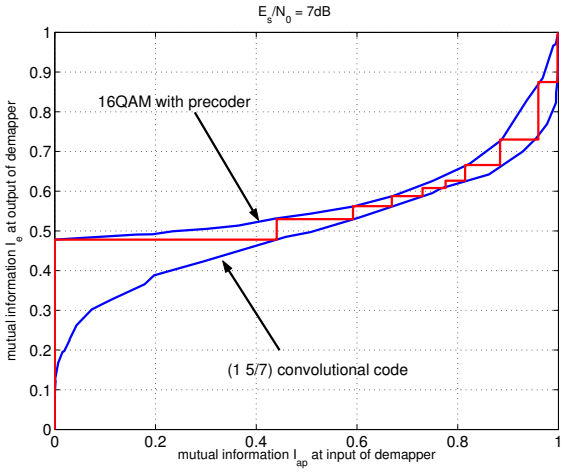

Figure 12: EXIT chart precoded QAM mappings as inner code in a BICM scheme.

4. COMPARISON OF EXIT CHARTS WITH OTHER METHODS FOR ANALYZING THE ITERATIVE PROCESS

The earliest attempt to visualize the behavior of a soft-in/soft-out decoder was given 1989 in [14] where the decoder of a convolutional code was treated as a nonlinear decimating filter which improves the signal–to–noise–ratio SNR. Instead of mutual information the SNR was used on the axes which is just a nonlinear axis transformation. Fig.13 taken with its caption from the original paper shows the SNR charts of three punctured codes with rates 3/4, 2/3 and 1/2 which are serially concatenated together with the trajectories of the decoding steps. Where the codes cross the rate one diagonal line a coding gain shows up much like the FM gain above the FM threshold in analog FM modulation. Only the feedback was missing, but this was 4 years before the discovery of turbo codes by Berrou et al.

Later Divsalar et al in [15] used the SNR charts for the evaluation of turbo codes. Other proposal used the mean, the

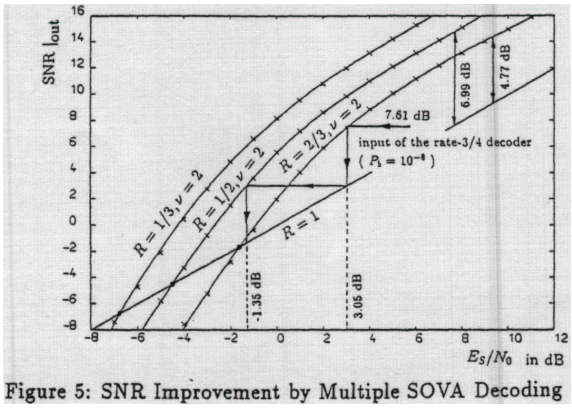

Figure 5: SNR Improvement by Multiple SOVA Decoding

Figure 13: SNR Chart for a serially concatenated punctured convolutional codes with rates 3/4, 2/3 and 1/2 taken from [14].

variance and the bit error rate as a figure of merit. In [12] we compared all these measures for visualizing the turbo behavior and found out that only two explain satisfactorily the behavior of the iterative process: The EXIT chart and the soft bit transfer ("SOBIT") chart, also called fidelity chart. These two charts reflect very closely the behavior of the iterative process. The SOBIT chart uses also the expectation over the soft bits which have real number values between -1 and +1.

$$\lambda = \tanh(L/2) = \mathrm{E}\{\tanh(L/2)\}$$

where the expectation is over the one parameter distribution Eqn.(16) for channel and a priori LLR. For unknown distributions as in case of L_E the expectation is over the measured distribution. In this case we better determine this value ranging between 0 and 1 by time averaging

$$\mathrm{E}\{\tanh(L/2)\} \approx \frac{1}{N}\sum_{n=1}^{N} x \cdot \tanh L/2$$

Examples for EXIT and SOBIT Charts are given in Fig.14 and Fig.15.

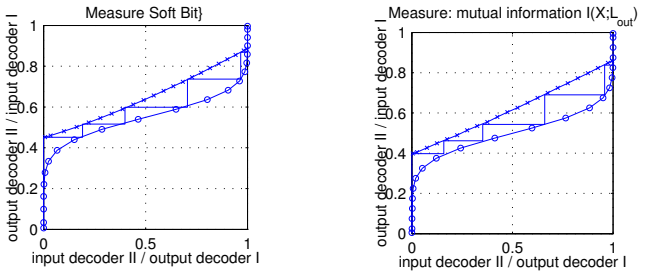

Figure 14: Serial concatenation with a multipath channel as inner code and an outer $M = 2$ convolutional code, $R = 1/2$

Why are the EXIT and the SOBIT charts so close? The SOBIT chart uses in the scheme of Fig.4 a nonlinear weighting function $\lambda = \tanh(L/2)$ whereas the EXIT chart uses the function (17)

$$1 - \log_2(1+e^{-L}) = \log_2(1+\lambda) \approx \frac{1}{\ln 2}\lambda = 1.4\lambda$$

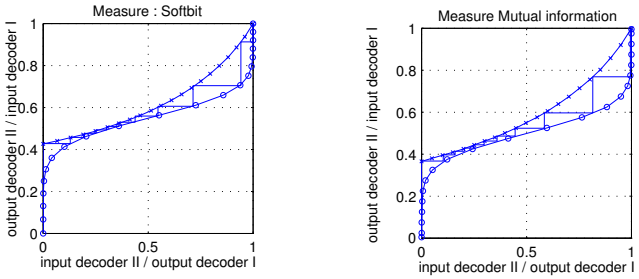

Figure 15: Serial concatenation with a DPSK modulator as inner code and an outer $M = 2$ convolutional code, $R = 1/2$

As shown in Fig.16 both weighting curves are very close for positive (no error)and small negative (error) L-values. Nevertheless the mutual information in the EXIT chart has the advantage of an information theoretic meaning measured in fractions of a bit. Another tool for analyzing the iterative

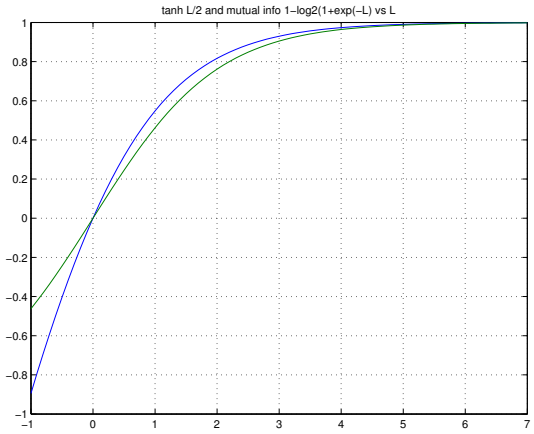

Figure 16: Comparison of the weighting functions in the EXIT and SOBIT curves

process is the density evolution described in [8] and [9]. This technique is mainly used for the analysis and optimization of regular and irregular low density parity check (LDPC) codes.

REFERENCES

[1] S. ten Brink, "Convergence behaviour of iteratively decoded parallel concatenated codes," *IEEE Trans. on Comm.*, vol. 49, Oct 2001.

[2] C. Berrou, A. Glavieux and P. Thitimajshima, "Near Shannon limit error-correcting coding and decoding: turbo-codes (1)," *Proc. IEEE International Conference on Communication (ICC)*, Geneva, Switzerland, May 1993, pp. 1064-1070.

[3] J. Lodge, R. Young, P. Hoeher, and J. Hagenauer, "Separable MAP 'filters' for the decoding of product and concatenated codes," *Proc. IEEE International Conference on Communication (ICC)*, Geneva, Switzerland, May 1993, pp. 1740-1745.

[4] J. Hagenauer, E. Offer and L. Papke, "Iterative decoding of binary block and convolutional codes," *IEEE*

Trans. on Information Theory, vol. 42, no.2, pp. 429–445, March 1996.

[5] I. Land, University of Kiel, private communication, 2003.

[6] I. Land et al, " Analytical results for EXIT charts for simple and LDPC codes", submitted to EUSIPCO, Wien, 2004. 2003.

[7] R. Gallager, "Low density parity check codes," *IRE Trans. on Information Theory*, vol. 8, pp. 21–28, January 1962.

[8] T. Richardson and R. Urbanke, "Design of capacity-approaching low density parity-check codes," *IEEE Trans. on Information Theory*, vol. 47, pp. 619–637, Feb 2001.

[9] S. Chung, T. Richardson and R. Urbanke, "Analysis of sum-product decoding of low-density-parity-check codes using a Gaussian approximation," *IEEE Trans. on Information Theory*, vol. 47, pp. 657–670, Feb 2001.

[10] S. ten Brink,G. Kramer,A, Ashikmin "Design of low-density parity check codes for multi-antenna modulation and detection," submitted to *IEEE Trans. on Comm.*, June 2002.

[11] M. Tüchler, R. Koetter, and A. Singer, "Turbo equalization: principles and new results," *IEEE Trans. on Comm.*, May 2002.

[12] M. Tüchler, S. ten Brink, and J. Hagenauer, "Measures for tracing convergence of iterative decoding algorithms," in *Proc. 4th IEEE/ITG Conf. on Source and Channel Coding*, Berlin, Germany, pp. 53–60, Jan 2002.

[13] M. Tüchler and J. Hagenauer, "EXIT charts of irregular codes," in *Proc. Conference on Information Science and systems, CISS 2002*, March 20-22, 2002.

[14] J. Hagenauer and P. Hoeher, "Concatenated Viterbi-decoding," in *Proceedings of the Fourth Joint Swedish-Soviet International Workshop on Information Theory*, Gotland, Sweden, September 1989, Studentlitteratur Lund, pp. 29–33, 1989.

[15] Divsalar, D., Dolinar, S., Pollara, F.: Low complexity Turbo-like codes, In: *Proc. International Symposium on Turbo Codes*, ENST, Bretagne, Frankreich, Sept. 2000, p. 78-80.

[16] Schreckenbach, F.; Görtz, N.; Hagenauer, J.; Bauch, G.: Optimized Symbol Mappings for Bit-Interleaved Coded Modulation with Iterative Decoding. - In:*2003 IEEE Global Telecommunications Conference (GLOBECOM 2003)*, San Francisco, Dezember 2003.